The Journal of Microbiology, June 2008, p. 300-308 Vol. 46, No. 3
DOI 10.1007/s12275-007-0212-6

Cyanobacterial Hybrid Kinase Sll0043 Regulates Phototaxis by Suppressing Pilin and Twitching Motility Protein

Bong-Jeong Shin[1], Jeehyun Oh[1], Sungsoo Kang[2], Young-Ho Chung[3], Young Mok Park[3], Young Hwan Kim[1], Seungil Kim[1], Jong Bhak[2], and Jong-Soon Choi[1]*

[1]Proteomics Team, Korea Basic Science Institute, Daejeon 305-333, Republic of Korea
[2]Korean BioInformation Center, KRIBB, Daejeon 305-806, Republic of Korea
[3]Systems Biology Team, Korea Basic Science Institute, Daejeon 305-333, Republic of Korea

(Received November 6, 2007 / Accepted March 14, 2008)

The unicellular cyanobacterium *Synechocystis* sp. PCC 6803 glides toward a light source through the interplay of positive phototaxis genes and proteins. In genetic analysis, the complete disruption of the hybrid sensory kinase *sll0043* produced negative phototaxis. Furthermore, Sll0043 was found to be a hub protein by *in silico* prediction of protein-protein interaction, in which Sll0043 was predominantly linked to seven two-component proteins with high confidence. To understand the regulation and networking of positive phototaxis proteins, the proteomic profile of the *sll0043* mutant was compared to that of wild-type. In the *sll0043* mutant, 18 spots corresponding to 15 unique proteins were altered by 1.3 to 59 fold; the spots were identified by 2-DE/MALDI-MS analysis. Down-regulated proteins in the *sll0043* null-mutant included chaperonins, superoxide dismutase, and phycocyanin β-subunit. In contrast, nine proteins involved in photosynthesis, translation, regulatory function, and other functions were up-regulated. In particular, a twitching motility protein (PilT1) was induced over 2-fold in *sll0043* mutant. Moreover, semi-quantitative and quantitative RT-PCR analysis revealed that pilin (*pilA1*), pili motor (*pilT1*), and pili switch gene (*pilT2*) were significantly increased in *sll0043* mutant. These results suggest that the hybrid kinase Sll0043 regulates positive phototaxis by suppressing the expression of pili biosynthesis and regulatory genes and through the interplay with positive phototaxis/motility two-component proteins.

***Keywords*:** cyanobacteria, two-component system, positive phototaxis, 2-DE/MALDI-MS, RT-PCR, protein-protein interaction network

Cyanobacteria are believed to be ancient photosynthetic organisms that appeared in the anoxygenic atmosphere 3.5 billion years ago (Douglas, 1998). During their adaptation to the extremely harsh earth environment, these organisms have evolved to sense light quality and quantity by photosensory receptors (Montgomery, 2007) and to display phototactic movement by type IV pili-dependent twitching motility system (Bhaya *et al*., 1999). The unicellular cyanobacterium *Synechocystis* sp. PCC 6803 (henceforth referred to as *Synechocystis*) is capable of exhibiting positive phototaxis and photokinesis that are defined as oriented movement toward a light source and increased scalar speed depending on light intensity irrespective of light direction, respectively (Choi *et al*., 1999; Chung *et al*., 2004). The phototactic movement of *Synechocystis* is thought to be a phenomenon driven by a series of signal cascades from light perception to behavioral response. The signal transduction that links photoperception and phototactic motility is attributed to the highly conserved bacterial two-component system in evolution (Mizuno *et al*., 1996). So far, more than 30 genes essential for phototactic motility (pili biogenesis, assembly and regulatory factors) have been identified by transposon-tagging and systematic gene disruption (Bhaya *et al*., 2004; Yoshihara and Ikeuchi, 2004). Among them, seven two-component genes that contain four response regulators and three histidine kinases are known to be related to phototactic gliding motility. In particular, three chemosensor-like gene loci were assigned as tax1 (*sll0038-sll0043*), tax2 (*sll1291-sll1296*), and tax3 (*slr1041-slr1044*, *slr0322*, *slr0073*) (Bhaya *et al.,* 2001). Two out of three of these gene clusters showed characteristic phototaxis and motility phenotypes: tax1 is functionally linked to positive phototaxis and tax3, which contains *slr0322* and *slr0073*, to motility. However, none of the tax2 mutants showed any alterations of the phototactic motility phenotype. Strikingly, the hybrid sensory kinase *sll0043* showed negative phototaxis when mutated (Bhaya *et al*., 2000; Yoshihara *et al*., 2000). Moreover, Sll0043 was expected to be a hub protein as it possesses 333 candidate interaction partners in the *Synechocystis*-specific protein-protein interaction database, SynechoNET (Kim *et al*., 2007). Among them, seven two-component proteins were predicted as high-confidence interaction partners.

In the present study, we attempted to characterize the function of Sll0043 that is responsible for positive phototaxis using 2D gel-based proteomics combined with relative quantitation of pilin mRNA expression, pili biosynthesis,

* To whom correspondence should be addressed.
(Tel) 82-42-865-3428; (Fax) 82-42-865-3419
(E-mail) jschoi@kbsi.re.kr

and pili regulation. In addition, we examined the protein interaction network of Sll0043 and its interaction partners related to positive phototaxis based on the SynechoNET database.

Materials and Methods

Strains, culture, transformation, and motility assay

The motile *Synechocystis* was grown in liquid BG-11 medium with 10 mM glucose at 28°C under the light intensity of 30 μmol/m^2/sec. Mutant *Synechocystis*, which contained the nonpolar spectinomycin-resistant gene (Sp^R) inserted in transcriptionally reverse direction at *sll0043*, was cultured on solidified BG11-agar plates with 10 μg/ml spectinomycin in BG11-media (Fig. 1A). Inactivation of the *sll0043* gene was performed as follows. In brief, the upstream flanking gene fragments of *sll0043* were amplified with forward primer UF; 5'-ATT AGC CAG GGA CAA GCG GA-3' and reverse primer UR; 5'-GGC GAG CAT CGT TTG TTC GCC CAG AAA ACT CGT AGG CGT GGT CA-3'. Likewise, the downstream flanking region of the *sll0043* gene was amplified with forward primer DF; 5'-TAA TGT CTA ACA ATT CGT TCA AGC TTA ACA GTT ATC ATT TTC CT-3' and reverse primer DR; 5'-CCG ACT TTT CTT CCA CCA CC-3'. By three-piece PCR fusion, the *sll0043*-upstream fragment, the nonpolar spectinomycin-cassette and the *sll0043*-downstream fragment were annealed at 50°C using the primer set of UF and DR. The resultant 2.5 kb DNA fragment was ligated into the TA-cloning vector. The *sll0043* knockout plasmid was transformed in competent *E. coli* DH5α cells. The transformed plasmid DNA was purified using the QIAGEN Plasmid DNA Midi-Prep Kit according to the manufacturer's protocol. The plasmid was introduced to transform the motile wild-type *Synechocystis* as previously explained (Chung *et al.,* 2001). The phototactic gliding phenotype was observed as previously described (Choi *et al.,* 1999).

Confirmation of knockout mutants by PCR analysis of genomic DNA

Wild-type *Synechocystis* and *sll0043*-inactivated mutant were cultivated to late exponential phase and the cells were harvested by centrifugation at 3,000×g for 15 min at 4°C. The cell pellets were resuspended in 200 μl of TEN buffer consisting of 10 mM Tris-HCl (pH 8.0), 50 mM EDTA, and 50 mM NaCl. Lysozyme (1 mg/ml) was added to the mixture and the subsequent solution was incubated at 37°C for 15 min. Five microliter of 10% (w/v) SDS and proteinase K (500 μg/ml) were added to the suspension, which was then incubated at 60°C for 45 min. After 200 μl of TEN buffer solution was added to the mixture, an equivalent volume of phenol (pH 8.0) was added and the mixture was incubated at room temperature for 5 min. After centrifugation, the supernatant solution was added to an equivalent volume of phenol/chloroform/isoamyl alcohol (10:9:1, v/v/v, pH 8.0) to extract the final supernatant. The genomic DNA from the supernatant was precipitated by the addition of 3 M sodium acetate (pH 5.0) and two-volumes of absolute ethanol. After centrifugation at 12,000×g for 30 sec, the pellet was washed with 70% ethanol, air dried and dissolved in sterile deionized water. The purified DNA was quantified by 0.8% agarose gel electrophoresis and stored at 4°C prior to use. To select for complete inactivation, the fragment containing

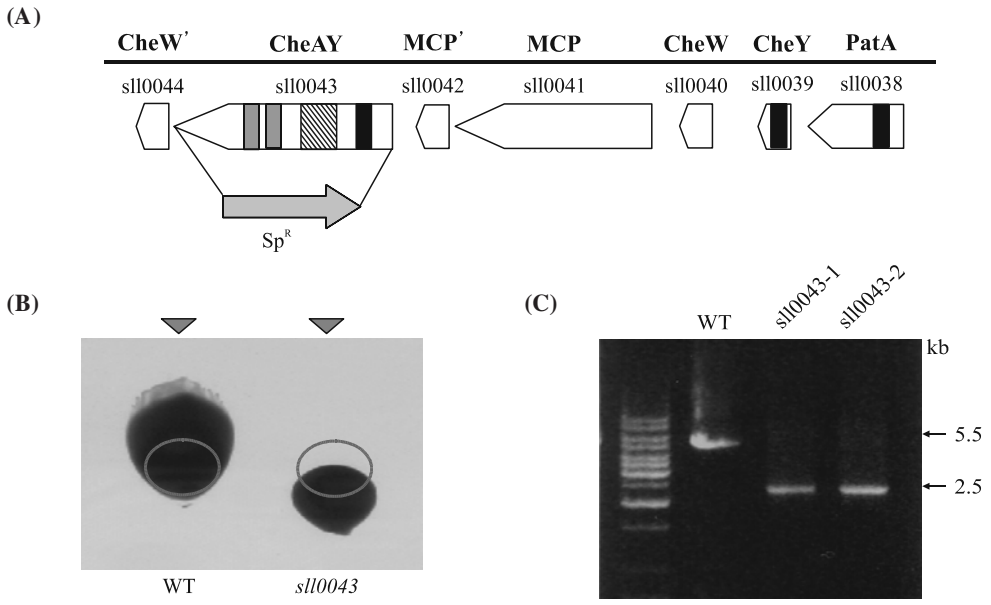

Fig. 1. Gene and domain organization of positive phototaxis-gene cluster (*sll0038-sll0044*). (A) The spectinomycin-resistance gene cassette was used to replace the *sll0043* ORF in the anti-parallel direction of transcription to generate the *sll0043* null-mutant. Gray box, Hpt-domain; Black box, RR-domain; Hatched box, ATPase domain. (B) Phototactic motility phenotype of wild-type and *sll0043*-null mutant. Five μl of each cell suspension was spotted on BG11-agar plates (0.4%) supplemented with 10 mM glucose. The tactic motility was observed for two days under lateral illumination in a culture tower at 28°C. Red circles indicate the initial spot position. (C) Genomic PCR analysis of wild-type and *sll0043* null-mutant was performed as described in 'Materials and Methods'.

sll0043-inserted spectinomycin-resistance was amplified from the genomic DNA of wild-type and *sll0043*-knockout mutants segregated at least five times.

Preparation of soluble protein fraction

Wild-type *Synechocystis* and *sll0043*-knockout mutant were harvested by centrifugation from 500 ml of BG11 culture media in mid-log phase (OD_{750}=0.5). The pelleted cells were resuspended in 5 ml of 10% (w/v) trichloroacetic acid : 90% acetone and broken by repetitive freezing and thawing with liquid nitrogen. After centrifugation at 18,000×g for 20 min at 4°C, the cell debris containing precipitated proteins was washed five times with 5 ml of ice-cold acetone. The pellet was solubilized in rehydration buffer (8 M urea, 2% CHAPS, 60 mM DTT, 0.5% IPG buffer). The insoluble proteins and cell debris were removed by centrifugation at 18,000×g for 20 min and the resulting supernatant was used in the proteome analysis. Before isoelectrofocusing, the protein was quantified by the Bradford method (Bradford, 1976).

2-DE analysis and image analysis

2-DE analysis of *Synechocystis* was conducted as described previously (Choi *et al*., 2000). In brief, the soluble proteins (200 μg) were applied on an immobilized pH gradient strip gel (pH 3∼10 non-linear, 18 cm) using the IPGphor system

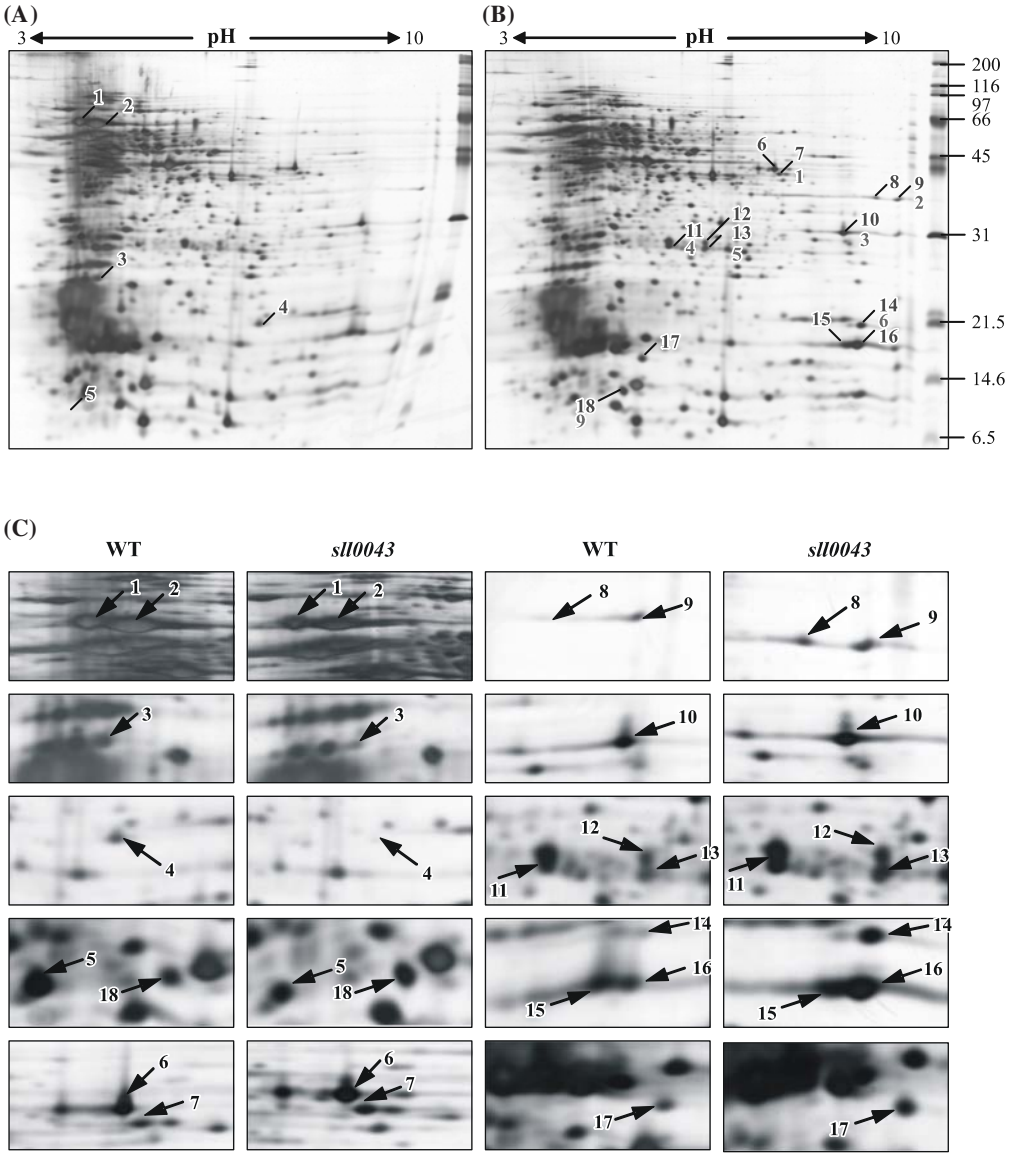

Fig. 2. Silver-stained 2DE-gels of (A) wild-type *Synechocystis* sp. PCC 6803 and (B) *sll0043*-deleted mutant. Whole soluble proteins were extracted from *Synechocystis* sp. cultured under constant light conditions (50 μmol/m^2/sec). The equivalent amount (200 μg) of proteins was separated on 2D-PAGE and stained with silver stain. The differentially expressed protein spots are indicated with arrows. The bars on the right indicate the location of the molecular size markers (kDa). (C) Magnified images of 2D-gels of wild-type and mutant are shown as up- or down-regulated spots.

(GE Healthcare, USA). In the first dimension, isoelectrofocusing was performed as follows: 300 V for 1 h, 500 V for 1 h, 1,000 V for 1 h, and 8,000 V for 10 h. The strip gel was equilibrated in buffer containing 50 mM Tris-HCl (pH 8.8), 6 M urea, 30% glycerol, 2% SDS, and a trace amount of bromophenol blue for 15 min at room temperature. In the second dimension, the equilibrated strip gel was run on 13% polyacrylamide SDS gel using a Hoefer Dalt (GE Healthcare, USA). Silver staining was carried out as described previously (Yan *et al*., 2000) using a silver staining kit (GE Healthcare). Silver-stained gels were scanned using Image Scanner (UMAX, Amersham-Pharmacia, Sweden) and the gel data were analyzed using Progenesis workstation version 2005 (Nonlinear Dynamics, UK). The protein spots were normalized by background subtraction, gel matching, and warping. Subsequently, the spot intensity of each detected spot was calculated as the spot volume. Up-regulated and down-regulated protein spots were confirmed by duplicate independent experiments.

Protein identification by MALDI-TOF TOF MS

In-gel digestion and protein identification by MALDI MS were conducted as described previously (Choi *et al*., 2000). Silver-stained protein spots were excised and destained with 15 mM potassium ferricyanide and 50 mM sodium thiosulfate. After the gel slices were rinsed with distilled water, the gel pieces were incubated in 100 mM ammonium bicarbonate and 10 mM DTT to reduce the protein disulfide bond and in 55 mM iodoacetamide and 100 mM ammonium bicarbonate to alkylate cysteine. Subsequently, the final dehydration of proteins in gel pieces was performed in a vacuum concentrator. The proteins were digested with sequencing grade trypsin (~1 μg) (Promega, USA) at 37°C, overnight, in 50 mM ammonium bicarbonate. Trypsinized gel pieces were extracted through repeated hydration-dehydration and sonication. Supernatants were transferred to new tubes and completely dried under vacuum for 6 h.

The resulting tryptic peptides were dissolved in 0.5% trifluoroacetic acid (TFA) solution, and then desalted using $ZipTipC_{18}$ (Millipore, USA) tips. Peptides were directly eluted onto MALDI target with α-cyano-4-hydroxy-cinnamic acid (10 mg/ml, dissolved in 0.5% TFA: 50% acetonitrile, 1:1, v/v). All mass spectra were acquired in reflection mode by a 4700 Proteomics Analyzer (Applied Biosystems, USA). All samples were irradiated with UV light (355 nm) from an Nd:YAG laser with a repetition rate of 200 Hz. Individual 1000 and 3000 laser shots were acquired and averaged to MS spectra and MS/MS spectra, respectively. The samples were analyzed at 25 kV source acceleration voltage with two-stage reflection in MS mode. In the MS/MS experi-

Table 1. List of proteins with altered expression level in *sll0043*-null mutant

Spot no.	Protein name	ORF no.	Access no.	Fold	MS MSMS	Coverage (%)	Measured Mr/pI	Theoretical Mr/pI
	Down-regulated proteins							
1	Chaperonin 60, GroEL2	Sll0416	AAA27284	-2.25	MSMS	14	66/4.0	57.8/5.02
2	GroEL1	Slr2076	BAA02180	-2.04	MSMS	8	66/4.2	57.7/4.97
3	Superoxide dismutase	Slr1516	NP_441347	-2.67	MSMS	13	25/4.2	21.7/4.90
4	Phycocyanin beta-subunit (CpcB)	Sll1577	AAA91032	-22.13	MSMS	32	22/7.2	18.1/4.98
5	10 kDa chaperonin (Cpn10), GroES	Slr2075	Q05971	-2.26	MSMS	53	10/5.4	10.8/5.06
	Up-regulated proteins							
6	Soluble hydrogenase 42 kDa subunit	Sll1559	NP_441695	+1.30	MSMS	22	44/7.5	40.7/6.76
7	Twitching motility protein (PilT1)	Slr0161	NP_441886	+2.03	MS	19	43/7.6	40.6/6.57
8	Phycocyanin associated linker protein (CpcC1)	Sll1580	NP_440549	+59.00	MSMS	30	37/9.4	32.5/9.35
9	Phycocyanin associated linker protein (CpcC1)	Sll1580	NP_440549	+1.65	MS	27	37/9.6	32.5/9.35
10	50S ribosomal protein L1 (Rpl1)	Sll1744	NP_440738	+1.36	MS	33	31/8.6	25.8/8.67
11	SOS function regulatory protein (LexA)	Sll1626	NP_441090	+1.51	MS	40	30/5.8	22.7/5.84
12	SOS function regulatory protein (LexA)	Sll1626	NP_441090	+1.89	MSMS	31	29/6.5	22.7/5.84
13	Transcription antitermination protein (NusG)	Sll1742	NP_440740	+1.60	MS	11	29/6.5	23.4/5.92
14	50S ribosomal protein L9 (Rpl9)	Sll1244	P42325	+20.80	MSMS	11	21/9.0	16.6/9.19
15	Photosystem I subunit II (PsaD)	Slr0737	NP_4408	+2.55	MSMS	30	18/8.7	15.6/8.94
16	Photosystem I subunit II (PsaD)	Slr0737	NP_4408	+7.45	MS	31	18/8.9	15.6/8.94
17	Hypothetical protein	Sll1307	NP_440960	+1.33	MSMS	12	18/5.3	17.8/6.06
18	Nitrogen regulatory protein P-II	Ssl0707	Q55247	+1.81	MS	39	16/5.1	12.4/6.34

ment, collision energy, which was defined as the potential difference between the source acceleration voltage (8 kV) and the floating collision cell (7 kV), was set to 1 kV. The MS spectra were processed using the Peak Explorer™ 3.0 (Applied Biosystems, USA) software. MS peaks with a signal-to-noise (S/N) ratio above 10 were listed, and the five strongest precursors with S/N ratio above 20 among the MS peaks were automatically selected for MS/MS acquisition. A mass filter was used to exclude noise, trypsin autolysis, keratin peaks and matrix cluster ions. MS spectra were externally calibrated with a standard peptide mixture of des-Arg Bradykinin, Angiotensin I, Glu-Fibrino-peptide B, Adrenocorticotropic hormone (ACTH) clip 1-17, ACTH clip 18-39, and ACTH clip 7∼38 and internally with two autolysis peaks of trypsin ($[M+H]^+$ = 842.5099 and 2211.1046).

Semi-quantitative RT-PCR and quantitative real-time PCR

Total RNA was isolated with TRIzol® (Invitrogen, USA) and RNase-free DNase (Promega, USA) according to the manufacturer's protocol. cDNA was synthesized using random primers and reverse transcriptase (Promega) in a 20 μl reaction volume with 1 μl of total RNA as a template. The expression of pili biosynthesis and regulatory genes was carried out with specific primers for *pilA1* (sense; 5'-GGG AGT CCG AAG CTA AAT CC-3', antisense; 5'-ATC AGG AGC TGG GAC TTC AA-3'), *pilT1* (sense; 5'-TAT GCA GAC CAT GGA ACA GG-3', antisense; 5'-ACG ACG TTT AGC GGC AAC-3'), *pilT2* (sense; 5'-AGT ATG GCT CCG GAA ACT CA-3', antisense; 5'-CTG GTG GGC TAG TGG GTA AA-3'), and *rnpB* (sense; 5'-TAA GAG CGC ACC AGC AGT ATC G-3', antisense; 5'-CAA ATT CCT CAA GCG GTT CCA C-3') as an internal control. PCR was performed with 1 μl of synthesized cDNA from the 20-μl reaction and 5 pmol of each primer set in a premixed PCR reaction kit (Bioneer, Korea) in the Thermocycler 9600 (Perkin Elmer, USA). PCR amplification was performed under the following conditions: initial denaturation at 94°C for 5 min, followed by 25∼40 cycles of 94°C for 30 sec, 54°C for 30 sec, and 72°C for 30 sec, and then extension at 72°C for 5 min.

Quantitative real-time (QRT) PCR components were the same as those used in RT-PCR except for HotStarTaq DNA polymerase (QIAGEN, Korea) and SyberGreen dye (QuantiTect™ SYBR® Green PCR Master Mix). QRT PCR was performed with 20 ng of synthesized cDNA from wild-type and mutant, 2 mM $MgCl_2$, 30 pM concentrations of specific primers and 1 unit of HotStarTaq DNA polymerase to a final volume of 20 μl in the Smart Cycler (Takara, Japan). PCR amplification was performed under the following conditions: initial denaturation at 95°C for 15 min, followed by 40 cycles of 95°C for 15 sec, 57°C for 30 sec, and 72°C for 30 sec. The relative cDNA quantities were determined from three independent experiments by comparing Ct (cycle of threshold) of test genes with that of normalized endogenous gene *rnpA* according to the QuantiTect™ SYBR® Green PCR Handbook. The statistical significance of relative quantitation data obtained from independent three experiments was assessed using unpaired Student's *t*-tests at $P<0.05$ and $P<0.01$.

Prediction of hybrid sensory kinase Sll0043-interacting proteins

In order to examine the protein-protein interaction network surrounding Sll0043 and Sll1694 (pilin), we analyzed the interaction partners linked to the query protein using the SynechoNET database (Kim *et al*., 2007). In brief, SynechoNET was designed for cyanobacterial domain-domain interactions as well as protein-level interactions using *Synechocystis* sp. PCC 6803. It integrated public protein-protein interaction databases that contained mutually complementary as well as redundant data. The interaction partners of Sll0043 (hybrid kinase) and Slr0161 (PilT1) were queried and displayed in the web pages of SynechoNET. Moreover, their protein interaction networks were dynamically visualized in the Java Applet viewer of SynechoNET.

Results

Phototactic motility of sll0043-knockout mutant

We isolated several altered phototaxis mutants from transposon-mutagenized library in *Synechocystis* Mutant Culture Collection. Detailed description on the transposon-mutagenesis procedure was referred to the previous our study (Chung *et al*., 2001). Among them, transposon 5-inserted clone at *sll0043* exhibited negative phototaxis on soft agar plates (data not shown). When any gene in tax1 was mutated, the mutant showed negative phototaxis as described previously (Yoshihara *et al*., 2000; Bhaya *et al*., 2001). The physical organization of the tax1 genes *sll0038-sll0044* showed sequence similarities to PatA-CheY-CheW-Mcp-Mcp'-CheAY-CheW' in order. By domain analysis, two Hpt domains with 120 amino acids in histidine kinase (HK) were found ex-

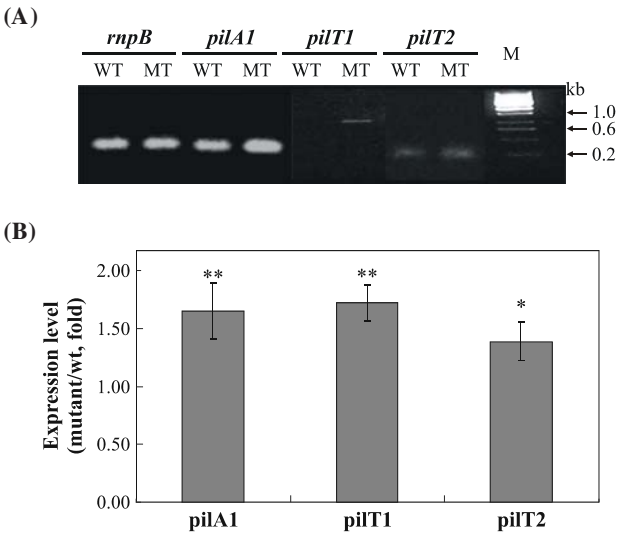

Fig. 3. Comparison of gene expression of pili biosynthesis and regulation. (A) Semi-quantitative RT-PCR of *pilA1*, *pilT1*, and *pilT2*. The PCR reaction conditions were described in Materials and Methods. WT, wild type; MT, *sll0043* knockout mutant; M, size marker. (B) Quantitative real-time PCR analysis of *pilA1*, *pilT1*, and *pilT2*. As a control, *rnpA* gene was used to obtain the ratios of pili genes versus *rnpA*. Data are presented as Mean±SD deviation of triplicate experiments. Asterisks * and ** denote $P<0.01$ and $P<0.05$, respectively.

clusively in Sll0043 (CheAY), whereas response regulator (RR) domains with 120 amino acids were present in Sll0038, Sll0039, and Sll0043 in the chemosensor-like operon (Fig. 1A). To confirm the negative phototaxis phenotype of the transposon *5*-insertion mutant of the hybrid sensory kinase *sll0043*, we generated a *sll0043*-null mutant by replacing the open reading frame (ORF) of *sll0043* with the spectinomycin resistance (Sp^r) cassette. The null mutant was constructed by fusion PCR (Wang *et al*., 2002). The upstream and downstream regions of the *sll0043* ORF were amplified with specific primers to generate an approximately 500 bp PCR amplicon. In particular, the upstream reverse and downstream forward primers of the flanking regions were designed to contain the complementary sequences matched with the Sp^r cassette. The *sll0043*-targeted mutant showed negative phototaxis on a soft agar plate (Fig. 1B). By genomic PCR analysis of independently segregated *sll0043* null-mutants, the original PCR length of the *sll0043* ORF (5.5 kb) shifted to 2.5 kb, supporting clear replacement by the Sp^r cassette (Fig. 1C).

Proteins regulated by hybrid sensory kinase Sll0043

To compare the proteomic profile of the hybrid sensory kinase *sll0043*-null mutant with that of wild-type, the soluble proteins were resolved on pH 3∼10 non-linear 2D-gels (Fig. 2). The intensities of 18 protein spots were altered when compared with control. All of the proteins of interest were identified by peptide mass fingerprinting and further peptide fragmentation using MALDI-TOF-TOF MS. In duplicate 2-DE analyses, we observed 15 proteins that exhibited altered expression levels (Fig. 2 and Table 1). The down-regulated proteins in the *sll0043*-null mutant were chaperonins (GroES, GroE1, and GroE2), superoxide dismutase (SOD), and phycocyanin β-subunit (CpcB). Remarkably, the expression level of CpcB decreased 22-fold in the mutant. Up-regulated proteins in the mutant were related to photosynthesis (phycocyanin-associated linker protein, CpcC1; photosystem I reaction center subunit II, PsaD), translation (50S ribosomal

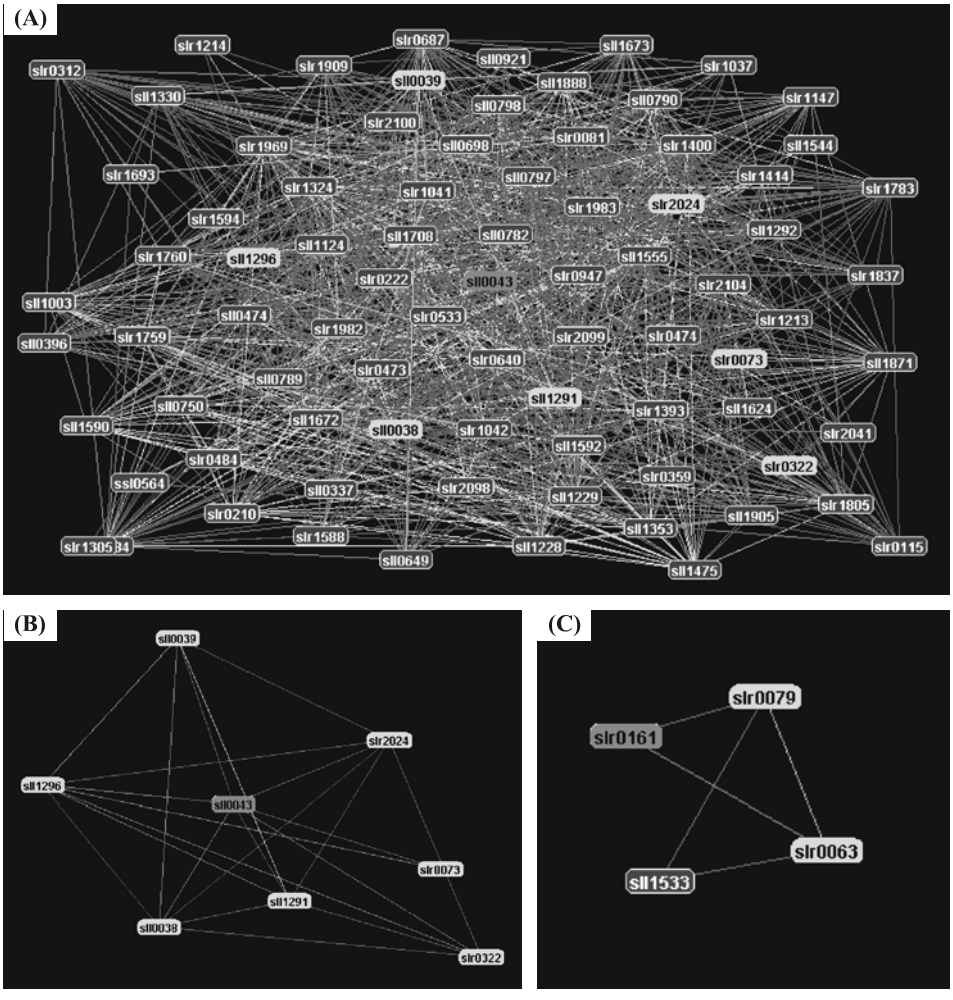

Fig. 4. Predicted protein-protein interaction network around hybrid kinase Sll0043 provided by SynechoNET. (A) A cluster of high-confidence interacting proteins containing Sll0043. The cluster was composed of 82 *Synechocystis* proteins that are mostly involved in regulatory functions. The bait protein Sll0043 was marked as green and its direct interaction partners as yellow. (B) High-confidence interaction partners of Sll0043. (C) High-confidence interaction partners of a twitching motility protein, Slr0161. The bait protein Slr0161 was marked as green and its direct interaction partners as yellow. Sll1533 encoded by *pilT2* was indirectly linked to Slr0161 via Slr0063 and Slr0079.

protein L1, Rpl1; 50S ribosomal protein L9, Rpl9), amino acid biosynthesis (nitrogen regulatory protein P-II, GlnB), regulatory function (SOS function, LexA; transcription antitermination protein, NusG) and others (soluble hydrogenase 42 kDa subunit; hypothetical protein). The expression levels of spots 8 (CpcC1), 14 (Rpl9), and 16 (PsaD) were highly increased by 59, 21, and 7 fold in the mutant, respectively. Interestingly, the expression level of twitching motility protein encoded by *slr0161* (*pilT1*, twitching motility) was increased 2 fold in the *sll0043* null-mutant, indicating that the hybrid sensory kinase Sll0043 suppresses the gene expression of PilT1.

Comparison of mRNA levels of pilA1, pilT1, and pilT2

In order to verify the up-regulation of twitching motility protein PilT1 observed in 2-DE/MS, the level of *pilT1* mRNA was examined and we extended to examine the levels of pilin (*pilA1*) and pili regulator (*pilT2*). The relative quantities of *pilA1*, *pilT1*, and *pilT2* were determined using RT-PCR and QRT-PCR analyses (Fig. 3). In the semi-quantitative RT-PCR analysis, the *pilA1* gene product was commonly observed within 25 cycles and the expression level of *pilA1* was slightly increased in the mutant. Contrary to the *pilA1* expression, the amplified PCR products of *pilT1* and *pilT2* were not observed with up to 35 cycles. When the PCR was extended to 40 cycles, a subtle difference in *pilT1* and *pilT2* levels was detected between wild-type and mutant. Presumably, the abundance of pili assembly and regulatory genes was relatively lower than that of pilin. The *pilT1* expression level was exclusively observed in the mutant with over 35 PCR cycles, whereas that of *pilT2* was almost the same in wild-type and mutant. In order to clarify the differential expression of pili-related genes, we performed an elaborate QRT-PCR analysis. QRT-PCR analysis clearly revealed that the transcript levels of *pilA1*, *pilT1*, and *pilT2* were significantly increased by up to 65% ($P<0.01$), 72% ($P<0.01$), and 39% ($P<0.05$), respectively, in the mutant compared to those in the wild-type. Thus, these results suggest that Sll0043 suppresses the expression of pili biosynthesis and regulatory genes to some extent.

Predicted interaction partners of Sll0043 and Slr0161

The high-confidence protein interaction network surrounding Sll0043 was predicted and visualized in the dynamic network viewer of SynechoNET (Fig. 4A). The network was composed of 82 *Synechocystis* proteins mostly involved in regulatory functions. Interestingly, two-component positive phototaxis proteins (Sll0038 and Sll0039) and motility proteins (Slr0073 and Slr0322) were directly linked to Sll0043 with high confidence (Fig. 4B). On the other hand, the pilin polypeptides (Sll1694, *pilA1*; Sll1695, *pilA2*; Slr1456, *pilA4*) (data not shown) and pili assembly and regulatory (Slr0161, *pilT1*; Sll1533, *pilT2*; Slr0063, *pilB1*; Slr0079, general secretion pathway protein E) proteins were independently separated as a satellite cluster (Fig. 4C). Therefore, the hybrid sensory kinase Sll0043 seems to be functionally linked to two-component phototaxis and motility proteins, but not directly associated with pilin and pili assembly and regulatory proteins.

Discussion

The phototrophic cyanobacterium *Synechocystis* sp. PCC 6803 has evolved to adapt to extreme environments by monitoring and transducing signal into the cell using a highly conserved two-component system. Cyanobacterial photomovement has been considered as an output response of the two-component system for optimal survival and growth. The two-component system consists of a sensory histidine kinase and its cognate response regulator (Stock *et al*., 2000). The sensory kinase contains an N-terminal domain that recognizes various stimuli, a histidine phospho-transfer (Hpt) domain, and an ATP-binding kinase domain (HK-ATPase). The partner response regulator contains a phospho-accepting receiver (RR) domain and a C-terminal effector domain. In the *Synechocystis* genome, 92 genes in the chromosomal DNA and two genes in the extra-chromosomal DNA (pSYSM, pSYSX) encode two-component systems: orthodox histidine kinases, response regulators, and hybrid sensory histidine kinase-possessing HK and RR domains in one primary sequence (Kaneko *et al*., 1996; Kaneko *et al*., 2003). In *E. coli* chemotaxis, the well-studied typical CheA-CheY two-component system is similar to that of *Synechocystis*, which harbors the unique positive phototaxis two-component system containing *sll0038-sll0044* (Yoshihara *et al*., 2000; Bhaya *et al*., 2001). Thus, *Synechocystis* cells can exhibit both positive and negative phototaxis in concerted coordination through the interplay of phototactic motility proteins and regulatory genes, i.e. even wild-type displays negative phototactic gliding movement under UV irradiation (Choi *et al*., 1999). In particular, the sensory hybrid kinase Sll0043, termed PixL, TaxAY1, or Hik18, presumably resides in a complicated positive phototaxis two-component signal transduction pathway as we observed negative phototaxis in the *sll0043*-null mutant (Fig. 1). With respect to the primary sequence characteristics, Sll0043 has two Hpts, one HK-ATPase, and one RR domain, whereas Sll1296 in tax2 has one Hpt, one HK-ATPase, and one RR domain, and Slr0322 has one Hpt-HK-ATPase domain and two RR domains (Bhaya *et al.,* 2001). Thus, there can be a complicated multiple phospho-relay directly or indirectly between Sll0043-HK and Sll0043-, Sll0038-, and Sll0039-RR domains and the unknown cross-talk between Sll0043 and other two-component systems.

In order to compare the physiological phenotypes such as cell growth and phototactic motility of *sll0043* mutant with those of wild-type, we constructed the null-mutant of *sll0043* using efficient three-piece PCR ligation; this method was designed to prevent residual sequences from showing a marginal phenotype after inactivation (Fig. 1). Various phenotypes of the same gene have been reported in the literature because of the different gene-knockout strategies, i.e. gene replacement with an antibiotic resistance cassette versus transposon insertion at *slr1443* (Kamei *et al*., 2002; Kim *et al*., 2004). The *sll0043*-null mutant showed a similar pattern of growth to wild-type under photoautotrophic and photoheterotrophic culture condition (data not shown), indicating that the *sll0043* gene is not essential for cellular survival. In order to investigate the effect of *sll0043* on the expression of genes involved in the positive phototaxis, we first attempted proteomic and transcriptional analysis of global

and targeted pili assembly and regulatory genes. In the global proteome profiles of *sll0043*-null mutant on 2D-gels, we did not observe any dramatic changes, but there were several differences in spot intensities based on duplicate gels. Chaperonins such as GroEL1 (Slr2076), GroEL2 (Sll0416), and GroES (Slr2075) and detoxifying enzyme SodB (Slr1516) were down-regulated in the *sll0043* mutant. This result was contrary to their up-regulation in response to the general stress of heat shock and high-light treatment (Glatz *et al*., 1997; Choi *et al*., 2000). Interestingly, the hybrid kinase Sll0043 positively regulates heat shock-responsive genes, whereas the global sensor kinase Slr1285, termed Hik34, negatively regulates the chaperonin genes (Slabas *et al*., 2006). In addition, GroEL2 and SodB were identified as targets that are negatively regulated by Hik34 and Rre1 (Slr1783) under salt and hyperosmotic stress (Shoumskaya *et al.,* 2005). Moreover, it is unusual that Sll0043 activates the expression of CpcB but inhibits that of CpcC1 under normal growth conditions. In *Synechocystis*, the *cpc* operon for the synthesis of phycobilisome contains *cpcB* (*sll1577*) and *cpcA* (*sll1578*) encoding phycocyanins, and *cpcC2* (*sll1579*), *cpcC1* (*sll1580*), and *cpcD* (*ssl3093*) encoding the rod linkers. It has been suggested that CpcC1 and CpcC2 were created by gene duplication in an ancestral strain and that CpcC1 became epistatic to CpcC2 (Ughy and Ajlani, 2004). Degradation of *cpcBA* transcript by high light was controlled by the membrane-bound histidine kinase NblS in *Synechococcus elongates* PCC 7942 (Van Waasbergen *et al*., 2002). In addition, Sll0043 may regulate the specific form of post-translationally modified proteins in phycobilisome light-harvesting and photosystem I complex since the relative acidic CpcC1 (spot 8, 59 fold) and basic PsaD (spot 16, 7.5 fold) were specifically increased in the mutant. Interestingly, ribosomal protein L9 (Rpl9) was specifically up-regulated by 21 fold in the mutant. Rpl9 is one of the proteins from the large ribosomal subunit in prokaryotes; Rpl9 is known to bind directly to the 23S rRNA and belongs to a family of ribosomal proteins grouped on the basis of sequence similarities (Hoffman *et al*., 1994). The sequence of *Synechocystis* Rpl9 was characterized compared to that of *Escherichia coli* and chloroplasts of Arabidopsis and pea (Malakhov *et al*., 1993). The regulation of specific ribosomal protein expression by histidine kinase is uncertain and remains to be elucidated.

Among the proteins that were up- or down-regulated by over 2 fold, a twitching motility protein PilT1 (spot 7) was detected in the *sll0043* null-mutant. Here, in order to verify the gene expression of pilin and pili assembly and regulator, we examined the relative quantities of *pilA1*, *pilT1*, and *pilT2* primary transcripts. Based on the motility/taxis phenotypes of pili genes that were previously conducted (Bhaya *et al*., 2000), we selected pilin (*pilA1*), a possible motor (*pilT1*), and taxis switch (*pilT2*) as the test genes. In contrast to PilA1, which is an abundant gene product, PilT1 and PilT2 seemed to be minor proteins; a subtle difference in the quantities of pili genes was detected between wild-type and *sll0043* mutant. From the RT-PCR and QRT-PCR analyses (Fig. 3), the transcript levels of *pilA1*, *pilT1*, and *pilT2* were significantly increased by up to 65% ($P<0.01$), 72% ($P<0.01$), and 39% ($P<0.05$), respectively. Thus, these results suggest that Sll0043 suppresses the expression of pili biosynthesis and regulatory genes to some extent. In a previous report, a *sll0043-3'* mutant exhibited negative taxis with normal expression of pilA1 while *sll0043-5'* mutant showed non-motile with 5 fold increase of pilA1 expression (Bhaya *et al*., 2001). Together with our finding that the full deletion of *sll0043* showed completely negative phototaxis and a little increase of pili assembly and regulatory genes, it can be concluded that Sll0043 plays a role of two different functions. Moreover, the *in silico* protein-protein interaction study using SynechoNET showed that the two-component positive phototaxis protein, Sll0043, specifically interacts with motility proteins (Slr0073 and Slr0322) and cognate response regulators (Sll0038 and Sll0039) as shown in Fig. 4. We confirmed the specific interaction between Sll0043 and Sll0038 or Sll0039 by yeast two-hybrid analysis (data not shown). It is noteworthy that the two-component positive phototaxis/motility protein clusters were unrelated to the pilin and pili regulation proteins in the protein-protein interaction network. Therefore, we believe that the hybrid sensory kinase Sll0043 is functionally linked to two-component phototaxis and motility proteins, but is not directly associated with pilin and pili assembly and regulatory proteins. Our finding is in good agreement with functional yeast two-hybrid analysis of Hik2/Rre1 and Hik10/Rre3 for sensing and signal transducing hyperosmotic stress (Paithoonrangsarid *et al*., 2004). To our knowledge, we are the first to apply the proteomic and quantitative transcriptional analysis to motility/taxis-related pili genes by Sll0043. In conclusion, we suggest that the hybrid kinase Sll0043 regulates phototaxis by suppressing pilin and twitching motility protein.

Acknowledgements

We thank Y.S. Jeon for helping with the construction of the plasmid vector. This project was supported by a grant (R01-2003-000-11720-0) from the Basic Research Program of Korea Science and Engineering Foundation and the Korea Basic Science Institute K-MeP (T27021) to J.S. Choi.

References

Bhaya, D. 2004. Light matters: phototaxis and signal transduction in unicellular cyanobacteria. *Mol. Microbiol*. 53, 745-754.

Bhaya, D., N. Watanabe, T. Ogawa, and A.R. Grossman. 1999. The role of an alternative factor in motility and pili formation in the cyanobacterium *Synechocystis* sp. PCC 6803. *Proc. Natl. Acad. Sci. USA* 96, 3188-3193.

Bhaya, D., N.R. Bianco, D. Bryant, and A.R. Grossman. 2000. Type IV pilus biogenesis and motility in the cyanobacterium *Synechocystis* sp. PCC 6803. *Mol. Microbiol*. 37, 941-951.

Bhaya, D., A. Takahashi, and A. Grossman. 2001. Light regulation of type IV pilus-dependent motility by chemosensor-like elements in *Synechocystis* sp. PCC 6803. *Proc. Natl. Acad. Sci. USA* 98, 7540-7545.

Bradford, M.M. 1976. A rapid and sensitive method for the quantitation of microgram quantities of protein utilizing the principle of protein-dye binding. *Anal. Biochem*. 72, 248-254.

Choi, J.S., D.S. Kim, J. Lee, S.J. Kim, S.I. Kim, Y.H. Kim, J. Hong, J.S. Yoo, K.H. Suh, and Y.M. Park. 2000. Proteome analysis of light-induced proteins in *Synechocystis* sp. PCC 68703: Identification of proteins separated by 2D-PAGE using N-terminal sequencing and MALDI-TOF MS. *Mol. Cells* 10, 705-711.

Choi, J.S., Y.H. Chung, Y.J. Moon, C. Kim, M. Watanabe, P.S. Song, C.O. Joe, L. Bogorad, and Y.M. Park. 1999. Photomovement of the gliding cyanobacterium *Synechocystis* sp. PCC 6803. *Photochem. Photobiol*. 70, 95-102.

Chung, Y.H., M.S. Cho, Y.J. Moon, J.S. Choi, Y.C. Yoo, Y.I. Park, K.M. Lee, K.W. Kang, and Y.M. Park. 2001. *ctr1*, a gene involved in a signal transduction pathway of the gliding motility in the cyanobacterium *Synechocystis* sp. PCC 6803. *FEBS Lett*. 492, 33-38.

Chung, Y.H., Y.M. Park, Y.J. Moon, E.M. Lee, and J.S. Choi. 2004. Photokinesis of cyanobacterium *Synechocystis* sp. PCC 6803. *J. Photosci*. 11, 89-94.

Douglas, S.E. 1998. Plastid evolution: origins, diversity, trends. *Curr. Opin. Genet. Dev.* 8, 655-661.

Glatz, A., I. Horvath, V. Varvasovszki, E. Kovacs, E. Torok, and Z. Vigh. 1997. Chaperonin genes of the *Synechocystis* PCC 6803 are differentially regulated under light-dark transition during heat stress. *Biochem. Biophys. Res. Commum*. 239, 291-297.

Hoffman, D.W., C. Davies, S.E. Gerchman, J.H. Kycia, S.J. Porter, S.W. White, and V. Ramakrishnan. 1994. Crystal structure of prokaryotic ribosomal protein L9: a bi-lobed RNA-binding protein. *EMBO J.* 13, 205-212.

Kamei, A., T. Yuasa, K. Orikawa, X.X. Geng, and M. Ikeuchi. 2002. Biochemical examination of the potential eukaryotic-type protein kinase genes in the complete genome of the unicellular cyanobacterium *Synechocystis* sp. PCC 6803. *DNA Res.* 9, 71-78.

Kaneko, T., Y. Nakamura, S. Sasamoto, A. Watanabe, M. Kohara, M. Matsumoto, S. Shimpo, M. Yamada, and S. Tabata. 2003. Structural analysis of four large plasmids harboring in a unicellular cyanobacterium, *Synechocystis* sp. PCC 6803. *DNA Res.* 10, 221-228.

Kaneko, T., S. Sato, H. Kotani, A. Tanaka, E. Asamizu, Y. Nakamura, N. Miyajima, N. Hirosawa, M. Sugiura, S. Sasamoto, T. Kimura, T. Hosouchi, A. Matsuno, A. Muraki, N. Nakazaki, M. Yamada, M. Yasuda, and S. Tabata. 1996. Sequence analysis of the genome of the unicellular cyanobacterium *Synechocystis* sp. PCC 6803 II. Sequence determination of the entire genome and assignment of potential protein-coding regions. *DNA Res.* 3, 109-136.

Kim, W.Y., S. Kang, B.C. Kim, J. Oh, S. Cho, J. Bhak, and J.S. Choi. 2007 SynechoNET: integrated protein-protein interaction database of a model cyanobacterium *Synechocystis* sp. PCC 6803. *BMC Bioinformatics* 9 (Suppl 1), S2O.

Kim, Y.H., Y.M. Park, S.J. Kim, Y.I. Park, J.S. Choi, and Y.H. Chung. 2004. The role of Slr1443 in pilus biogenesis in *Synechocystis* sp. PCC 6803: involvement in post-translational modification of pilins. *Biochem. Biophys. Res. Commun*. 315, 179-186.

Malakhov, M.P., H. Wada, D.A. Los, T. Sakamoto, and N. Murata. 1993. Structure of a cyanobacterial gene encoding the 50S ribosomal protein L9. *Plant Mol. Biol*. 21, 913-918.

Mizuno, T., T. Kaneko, and S. Tabata. 1996. Compilation of all genes encoding bacterial two-component signal transducers in the genome of the cyanobacterium, *Synechocystis* sp. strain PCC 6803. *DNA Res*. 3, 407-414.

Montgomery, B.L. 2007. Sensing the light: photoreceptive systems and signal transduction in cyanobacteria. *Mol. Microbiol.* 64, 16-27.

Paithiinrangsarid, K., M.A. Shoumskaya, Y. Kanesaki, S. Satoh, S. Tabata, D.A. Los, V.V. Zinchenko, H. Hayashai, M. Tanticharoen, I. Suzuki, and N. Murata. 2004. Five histidine kinases perceive osmotic stress and regulate distinct sets of genes in *Synechocystis. J. Biol. Chem*. 279, 53078-53086.

Shoumskaya, M.S., K. Paithoonrangsarid, Y. Kanesaki, D.A. Los, V.V. Zinchenko, M. Tanticharoen, I. Suzuki, and N. Murata. 2005. Identical Hik-Rre systems are involved in perception and transduction of salt signals and hyperosmotic signals but regulate the expression of individual genes to different extents in *Synechocystis. J. Biol. Chem*. 280, 21531-21538.

Slabas, A.R., I. Suzuki, N. Murata, W.J. Simon, and J.J. Hall. 2006. Proteomic analysis of the heat shock response in *Synechocystis* PCC 6803 and a thermally tolerant knockout strain lacking the histidine kinase 34 gene. *Proteomics* 6, 845-864.

Stock, A.M., V.L. Robinson, and P.N. Goudreau. 2000. Two-component signal transduction. *Annu. Rev. Biochem*. 69, 183-215.

Ughy, B. and G. Ajlani. 2004. Phycobilisome rod mutants in *Synechocystis* sp. strain PCC6803. *Microbiology* 150, 4147-4156.

Wang, H.L., B.L. Pstier, and R.L. Burnap. 2002. Optimization of fusion PCR for *in vitro* construction of gene knockout fragments. *Biotechnique* 33, 26-30.

Van Waasbergen, L.G., N. Dolganov, and A.R. Grossman. 2002. nblS, a gene involved in controlling photosynthesis-related gene expression during high light and nutrient stress in *Synechococcus elongatus* PCC 7942. *J. Bacteriol*. 184, 2481-2490.

Yan, J.X., R. Wait, T. Berkelman, R.A. Harry, J.A. Westbrook, C.H. Wheeler, and M.J. Dunn. 2000. A modified silver nitrate staining protocol for visualization of proteins compatible with matrix-assisted laser desorption/ionization and electrospray ionization-mass spectrometry. *Electrophoresis* 21, 3666-3672.

Yoshihara, S. and M. Ikeuchi. 2004. Phototactic motility in the unicellular cyanobacterium *Synechocystis* sp. PCC 6803. *Photochem. Photobiol. Sci*. 3, 512-518.

Yoshihara, S., F. Suzuki, H. Fujita, X.X. Geng, and M. Ikeuchi. 2000. Novel putative photoreceptor and regulatory genes required for the positive phototactic movement of the unicellular motile cyanobacterium *Synechocystis* sp. PCC 6803. *Plant Cell Physiol*. 41, 1299-1304.